

# Thermopower of SnTe from Boltzmann Transport Calculations

David J. Singh

*Materials Science and Technology Division, Oak Ridge National Laboratory  
 Oak Ridge, TN 37831-6114, USA. singhdj@ornl.gov*

Received Day Month Year

Revised Day Month Year

The doping and temperature dependent thermopower of SnTe is calculated from the first principles band structure using Boltzmann transport theory. We find that the *p*-type thermopower is inferior to PbTe consistent with experimental observations, but that the *n*-type thermopower is substantially more favorable.

*Keywords:* SnTe, thermoelectrics, thermopower

## 1. Introduction

Thermoelectrics offer a useful technology for small scale cooling and power generation applications. The performance of such devices is limited by a materials and temperature dependent dimensionless figure of merit,  $ZT = \sigma S^2 T / \kappa$ , where  $T$  is temperature,  $\sigma$  is the electrical conductivity,  $S$  is the thermopower and  $\kappa$  is the thermal conductivity, which is generally the sum of lattice and electronic components,  $\kappa_l$  and  $\kappa_e$ . There has been considerable recent interest in finding new thermoelectric materials.<sup>1; 2</sup>

In this regard, there have been recent developments in PbTe based materials, particularly with heavy Tl doping<sup>3</sup> and via alloying with small amounts of AgSbTe<sub>2</sub>, which leads to a nanostructured material denoted LAST.<sup>4</sup> Both of these materials have  $ZT$  well above unity. In the LAST material this arises primarily because of a reduction in thermal conductivity associated with the nanostructuring,<sup>4</sup> and possibly connected with the nearness of the phase to a ferroelectric instability.<sup>5</sup> In PbTe:Tl the high  $ZT$  is instead caused by an enhanced thermopower at high Tl doping levels. GeTe alloyed with small amounts of AgSbTe<sub>2</sub> is also a

very high performance thermoelectric, with a  $ZT$  that exceeds 1.2 at high temperature.<sup>1; 6</sup> There are, however, certain disadvantages to these materials. Specifically, the use of Pb limits applications due to environmental and regulatory issues, while Ge is a very costly material. On the other hand, Sn is both environmentally benign and inexpensive. This suggests investigation of SnTe, which occurs in the same structure.

In fact, there have been a number of experimental investigations of the thermoelectric performance of SnTe with various doping strategies. One difficulty is that SnTe forms with a high concentration of native defects, particularly Sn vacancies, which are difficult to avoid because of the shape of the liquidus line in the Sn-Te phase diagram.<sup>7</sup> This leads to difficult to control high *p*-type carrier concentrations. These can be compensated by alloying with Bi. However, even then samples are still generally *p*-type.<sup>8; 9</sup>

Furthermore, experimental investigations of *p*-type SnTe have invariably found low values of  $ZT$  in comparison to PbTe.<sup>10</sup> This can be traced to the behavior of  $S(T)$ . The thermal conductivity of SnTe,  $\kappa \sim 2$  W/m K, is similar to that of GeTe and PbTe, and can be strongly reduced by alloying.<sup>10</sup>

However,  $S(T)$  is lower than in comparable PbTe.<sup>8</sup> This leads to a much lower  $ZT$  in SnTe as compared with PbTe. Interestingly, an enhancement of the thermopower was found at high carrier concentrations between  $\sim 2 \times 10^{20} \text{ cm}^{-3}$  and  $10^{21} \text{ cm}^{-3}$ ,<sup>8</sup> similar to what occurs in Tl doped PbTe, although in PbTe this is at lower carrier density.<sup>11</sup>

## 2. Structure and Methods

We applied Boltzmann transport theory within the constant scattering time approximation (CSTA) to the first principles electronic structure as obtained within density functional theory using the general potential linearized augmented plane wave (LAPW) method as implemented in the WIEN2K code,<sup>12</sup> similar to our prior work on PbTe and  $\text{PbBi}_2\text{Te}_4$ .<sup>11; 13</sup> Spin-orbit was included in all the calculations. We used well converged basis sets and Brillouin zone samplings with LAPW sphere radii of 2.0 Bohr for both Sn and Te. The CSTA allows the thermopower to be directly calculated from the band structure as a function of carrier concentration and  $T$  with no adjustable parameters.<sup>14; 15</sup> The needed integrals were obtained using the BoltzTraP code.<sup>16</sup> One complication is that the band gaps of semiconductors are typically underestimated in density functional calculations. For small band gap materials this will lead to bipolar conduction and reduce the thermopower at high temperatures especially when the carrier density is low. We used the Engel-Vosko generalized gradient approximation (GGA) to avoid this.<sup>17</sup> Unlike standard GGA's, this functional is optimized to reproduce the exchange-correlation potential rather than the total energy, and as a result gives improved band gaps.

While PbTe is almost ferroelectric, both SnTe and GeTe are ferroelectric, with Curie temperatures,  $T_C$  of 120 K and  $\sim 700$  K, respectively. SnTe occurs in the cubic NaCl structure above  $T_C$  and is rhombohedral below. Here we present results from 300 K up, and so we use the NaCl structure with the experimental lattice parameter,  $a=6.303 \text{ \AA}$ .

## 3. Electronic Structure

The calculated band structure is shown in Fig. 1. It is similar to prior relativistic calculations<sup>18</sup> and in particular shows a direct gap at the  $L$  point, with non-parabolic bands that become effectively

heavier as the chemical potential moves away from the band edges. Our calculated band gap with the Engel-Vosko GGA is  $E_g=0.17 \text{ eV}$ , which is less than the value of 0.30 eV obtained by the same procedure applied to PbTe.<sup>11</sup> The calculated gap is in good agreement with the experimental room temperature value of 0.18 eV<sup>19</sup> (note that at low  $T$  SnTe has a different ferroelectric crystal structure).

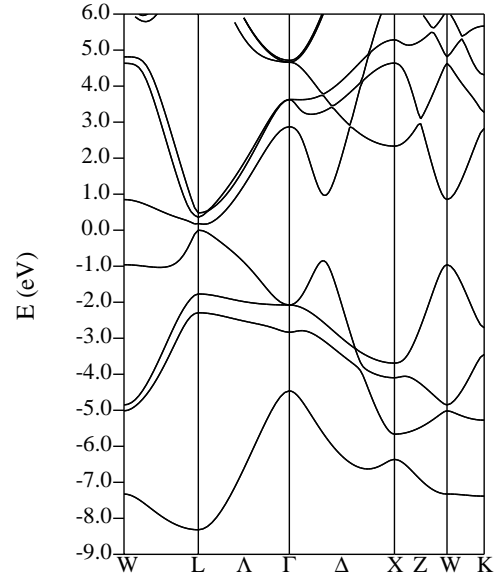


Fig. 1. Band structure of cubic SnTe obtained with the Engel-Vosko GGA, including spin-orbit.

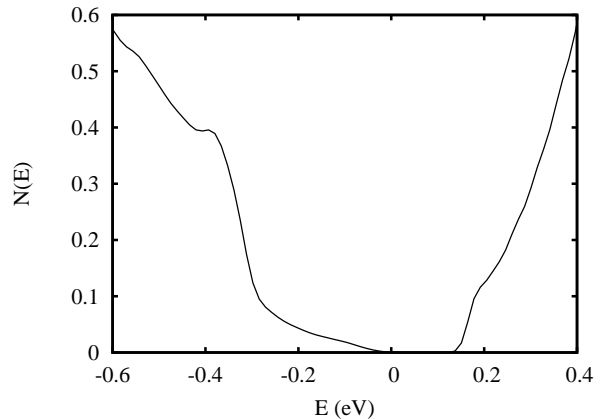


Fig. 2. Electronic DOS of SnTe.

The calculated electronic density of states (DOS) in the region near the band edges is shown in Fig. 2. Similar to PbTe,<sup>11</sup> it shows a light mass behavior at the valence band edge with a strong upturn at  $\sim 0.3 \text{ eV}$ . This arises for the same reason, i.e. connection of the  $L$ -point pockets along the approximately  $[001]$  oriented directions connecting

them. This is qualitatively consistent with the band structure model developed by Allgaier and Houston based on magnetotransport measurements.<sup>20</sup> However, this upturn in the DOS is not as strong as in PbTe. Also, one may note in the band structure that the dispersion of the conduction bands from  $L$ - $W$  is weaker in SnTe. This leads to a higher DOS near the conduction band edge, i.e. higher effective band mass for  $n$ -type. Finally, the DOS in the conduction bands has structure at  $\sim 0.2$  eV above the edge. This comes from the second and third conduction bands which have their minima at  $L$  (note that there is a small splitting between these minima). These bands are more dispersive than the lowest conduction band.

Thus, SnTe behaves as a material with lighter bands than PbTe for  $p$ -type and heavier bands than PbTe for  $n$ -type. These differences are reflected in the behavior of the thermopower.

#### 4. Thermopower

Our main results are presented in Figs. 3 and 4, which show the doping dependence of  $S(T)$  for  $p$ -type and  $n$ -type, respectively. We show data from 300 K to 800 K (the liquidus temperature is 1078 K<sup>7</sup>). As may be seen, the  $p$ -type thermopowers are inferior to PbTe.

It can be shown that when the Wiedemann-Franz relation holds  $ZT = rS^2/L$ , where  $L$  is the Lorentz number and  $r = \kappa_e/\kappa < 1$ . Taking the standard value of  $L$ ,  $S > 157 \mu\text{V/K}$  is required for  $ZT=1$ , even assuming that  $\kappa_l$  is negligible. Based on this and the results in Fig. 3 it would seem that the only regimes where  $p$ -type SnTe could have a high  $ZT$  are (1) at high carrier concentrations ( $\sim 10^{20} \text{ cm}^{-3}$ ) and very high temperatures, where the material is known to be prone to Sn vacancy formation and (2) near ambient  $T$  with a low carrier concentration  $\sim 2 \times 10^{18}$ , and then only if very high mobility samples can be prepared or the thermal conductivity suppressed (e.g. by alloying). Interestingly, we do find an enhancement of the thermopower in the range from  $10^{20} \text{ cm}^{-3}$  to  $10^{21} \text{ cm}^{-3}$  as in experiment. However, unlike PbTe<sup>11</sup>, the resulting values of  $S$  are too low for high  $ZT$ .

The situation for  $n$ -type is much more interesting. At very low  $n$ -type carrier densities ( $\sim 10^{18} \text{ cm}^{-3}$ ) and very high temperatures, the combination of light valence bands and heavy conduction bands leads to a positive  $T$  independent thermopower due to bipolar conduction. At more realistic doping lev-

els the thermopower is much higher than for  $p$ -type, and importantly  $S(T)$  is also substantially higher than in  $n$ -type PbTe and remains high even at very high doping levels in excess of  $10^{20} \text{ cm}^{-3}$ , depending on  $T$ .

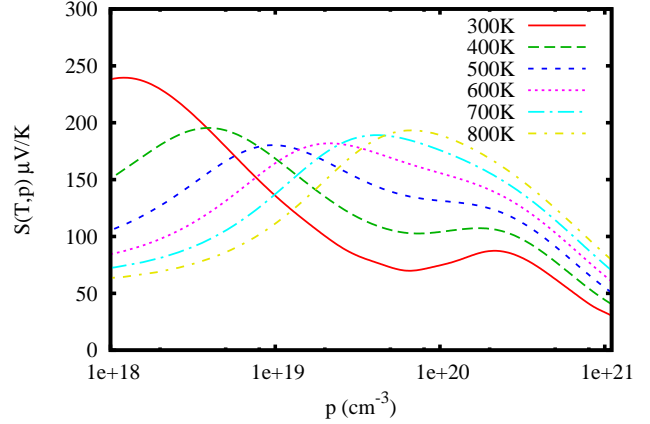


Fig. 3. Calculated doping dependence of  $S(T)$  for  $p$ -type SnTe.

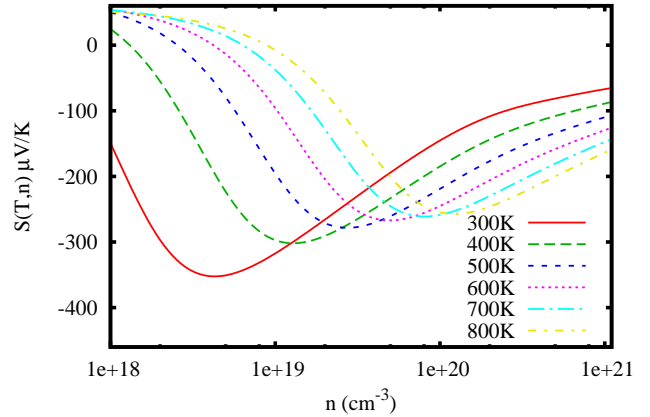


Fig. 4. Calculated doping dependence of  $S(T)$  for  $n$ -type SnTe.

#### 5. Summary and Conclusions

To summarize, we calculated  $S(T)$  for SnTe as a function of carrier concentration and temperature. We find that the values of  $S$  are substantially inferior to those of PbTe for  $p$ -type, consistent with existing experimental data showing inferior thermoelectric performance. On the other hand, we find that the behavior of  $S$  for  $n$ -type is significantly superior to that of  $n$ -type PbTe. Considering that the two compounds have similar lattice thermal conductivities this indicates that optimized  $n$ -type SnTe could have superior thermoelectric performance to

*n*-type PbTe. However, as mentioned, SnTe almost invariably forms as *p*-type material due to the shape of the liquidus line in the Sn-Te binary phase diagram, which results in Sn deficient samples. This can be controlled in part by annealing or Bi doping.<sup>7; 8</sup> However, there has been little recent experimental work on SnTe, perhaps because of the known poor performance of *p*-type material. Perhaps modern doping strategies, such as controlled co-doping (possibly including the Te site, e.g. alloying with both Bi and Se) could yield *n*-type material. If so, based on the present results it will be very interesting to determine the thermoelectric performance of heavily doped *n*-type SnTe.

## Acknowledgments

We are grateful for helpful discussions with David Parker. This research was sponsored by the U.S. Department of Energy, Office of Science, Materials Sciences and Engineering Division.

## References

1. G. J. Snyder and E. S. Toberer, *Nature Materials* **7**, 105 (2008).
2. J. R. Sootsman, D. Y. Chung and M. G. Kanatzidis, *Angew. Chem. Int. Ed.* **48**, 8616 (2009).
3. J. P. Heremans, V. Joavovic, E. S. Toberer, A. Saramat, K. Kurosaki, A. Charoenphakdee, S. Yamanaka and G. J. Snyder, *Science* **321**, 554 (2008).
4. K. F. Hsu, S. Loo, F. Guo, W. Chen, J. S. Dyck, C. Uher, T. Hogan, E. K. Polychroniadis and M. G. Kanatzidis, *Science* **303**, 818 (2004).
5. J. An, A. Subedi and D. J. Singh, *Solid State Commun.* **148**, 417 (2008).
6. B. A. Cook, M. J. Kramer, X. Wei, J. L. Harringa and E. M. Levin, *J. Appl. Phys.* **101**, 053717 (2007).
7. R. F. Brebrick, *J. Phys. Chem. Solids* **24**, 27 (1963).
8. R. F. Brebrick and A. J. Strauss, *Phys. Rev.* **131**, 104 (1963).
9. M. A. Tamor, H. Holloway, R. M. Ager, C. A. Gierczak and R. O. Carter, *J. Appl. Phys.* **61**, 1094 (1987).
10. C. C. Wu, N. J. Ferng and H. J. Gau, *J. Cryst. Growth* **304**, 127 (2007).
11. D. J. Singh, *Phys. Rev. B* **81**, 195217 (2010).
12. P. Blaha, K. Schwarz, G. Madsen, D. Kvasnicka and J. Luitz, *WIEN2k, An Augmented Plane Wave + Local Orbitals Program for Calculating Crystal Properties* (K. Schwarz, Tech. Univ. Wien, Austria) (2001).
13. L. Zhang and D. J. Singh, *Phys. Rev. B* **81**, 245119 (2010).
14. D. J. Singh and I. I. Mazin, *Phys. Rev. B* **56**, R1650 (1997).
15. K. P. Ong, D. J. Singh and P. Wu, *Phys. Rev. Lett.* **104**, 176601 (2010).
16. G. K. H. Madsen and D. J. Singh, *Comput. Phys. Commun.* **175**, 67 (2006).
17. E. Engel and S. H. Vosko, *Phys. Rev. B* **47**, 13164 (1993).
18. Y. W. Tung and M. L. Cohen, *Phys. Rev.* **180**, 823.
19. L. M. Rogers, *Brit. J. Appl. Phys.* **1**, 845 (1968).
20. R. S. Allgaier and B. Houston, *Phys. Rev. B* **5**, 2186 (1972).